JOURNAL OF MATERIALS SCIENCE **34** (1999) 4501–4509

Strength degradation of Si_3N_4 exposed to simulated gas turbine environments

M. CARRUTH, D. BAXTER, J. DUSZA*
European Commission—Joint Research Centre, Institute for Advanced Materials, 1755 ZG Petten, The Netherlands
E-mail: BAXTER@JRC.NL

Silicon nitride, sintered with the aid of alumina and yttria, was exposed at 1000 °C to two different simulated gas turbine environments. The composition of the reaction gas was varied by delivering either a high or low sulphur fuel into a burner rig. The characteristics of the corrosion product varied markedly with the sulphur content of the fuel. The extent of silicon nitride degradation was examined by two techniques: weight change and 4-point flexural strength. Strength measurements were conducted both at room temperature and at 1000 °C. Whereas the weight gain information revealed that corrosion was enhanced in the low sulphur combustion gas, the strength of the corroded silicon nitride did not vary significantly from that of the as-received material. Scanning electron microscopy of the fracture surfaces was utilised to identify the fracture origins in the as-received and corroded samples. Strength, even after corrosion, was controlled primarily by defects introduced during manufacture.

1. Introduction

The application of structural ceramics in power generation systems has been one of the major driving forces behind the extensive research performed on silicon based ceramics. The inherent low density and high temperature stability of silicon nitride can permit major weight savings and higher operating temperatures to allow greater energy efficiency and a reduction in the level of harmful emissions.

The interest in silicon nitride ceramics for use in high temperature applications has prompted closer investigation of the materials' interaction with aggressive environments. Silicon nitride's excellent oxidation resistance in pure environments is attributed to the formation of a self-healing layer of silica (SiO_2) that restricts oxygen transport. Particular attention has been paid to the behaviour of silicon nitride in simulated gas turbine environments [1–3].

In a gas turbine, airborne sodium reacts with sulphur present in the fuel to form sodium sulphate (Na_2SO_4), which may under certain conditions condense onto cooler engine components. The corrosion process is generally regarded to involve the dissolution of the normally protective silica layer by the molten salt. Oxygen transport is enhanced through the subsequent liquid silicate that forms, permitting accelerated oxidation of the ceramic substrate and degradation of the material's properties. Special importance is attached to the Na_2O activity of the salt deposit since it determines the thermodynamic conditions for the dissolution of silica [4, 5]. Dissolution is kinetically favoured when a high Na_2O activity exists. This may be achieved by lowering the partial pressure of SO_3, which is set by the sulphur content of the fuel.

$$Na_2SO_4(l) = Na_2O(s) + SO_3(g) \quad (1)$$

However, developing ceramic gas turbines are expected to operate at temperatures above the dew point of sodium sulphate. It is therefore important to establish the interaction of Si_3N_4 with salt vapours. Previous work in this laboratory has highlighted the effect of the sulphur concentration of simulated combustion gases on the physical and chemical properties of the reaction product formed on silicon carbide (SiC) [6]. Lowering the P_{SO_3} resulted in higher levels of sodium in the oxide and led to higher rates of degradation. The current study differs from earlier investigations by aiming to establish the effect of sulphur on the strength of silicon based ceramics exposed to salt vapours.

Several techniques have been used to study the behaviour of silicon nitride for gas turbine applications. Crucible tests [4] and furnace studies [7] are relatively inexpensive and simple to perform, the experimental conditions are easily reproduced and there is good control over many of the operating parameters. However the primary disadvantage of these methods is that they do not adequately model a gas turbine environment [8].

Burner rigs are accepted to simulate gas turbine environments better than crucible or furnace tests. The combined effects of corrosion, erosion and thermal cycling can be simultaneously or independently studied.

* *Permanent address*: Institute of Materials Research, Watsonova 47, 043 53 Kosice, Slovakia.

Candidate materials are exposed to the dynamic gases from the combustion of fuels, to which salts or other contaminants may be added.

Although few standard methodologies for corrosion testing exist, guidelines are available for performing burner rig tests [9]. This procedure was developed from knowledge of the critical parameters affecting corrosion when salt deposition occurs, and offers a foundation from which standard burner rig corrosion procedures can be evolved.

Standard corrosion studies are only beneficial when they are supplemented with standard methods to evaluate corrosion. Various techniques are used to define the extent of corrosion, but in each case standard procedures have not been established. The change in sample weight per surface area is perhaps the most frequently used method of assessing corrosion [10–12]. This information is obtained quickly and easily to provide the details on the overall effects of oxidation. However, weight change data can be misleading, especially when oxidation involves simultaneous processes, or when the attack morphology is non-uniform.

Material loss is an emerging method of assessing corrosion [13] and involves comparing the section thickness after exposure with the material's original dimensions. The technique allows for the generation of a large data set and by performing statistical analysis, the average and maximum extent of damage can be calculated. However, great uncertainty exists in the ability of this technique to accurately define corrosion. Unknown errors arising from poor sample preparation and dimensional characterisation can generate large discrepancies between the actual and measured material loss during corrosion.

Measurement of a mechanical property may more appropriately define the extent of corrosion since ceramics inevitably fail by the effects of material degradation on strength, creep or fatigue. Strength is perhaps the most reasonable property to measure since testing is relatively quick and simple to perform, and strength limiting failure mechanisms are well understood. Evaluating corrosion by strength measurement also has the advantage of being sensitive to the mode of attack, unlike other techniques [7], such as weight change. Thus strength measurement allows the investigation of the influence of localised corrosion on the material's performance. In fact, strength measurements can highlight a significant difference between the oxidation resistance of materials that show similar weight gain [14]. Therefore, strength measurement may provide a better assessment of the extent of oxidation under certain circumstances.

Considering these advantages of evaluating corrosion by strength determination, it may be surprising that relatively few studies have applied this technique. This is perhaps a consequence of the many samples that must be destructively tested to obtain representative data. When strength testing is used as a tool to define corrosion, room temperature 4-point flexural strength measurement is generally the most commonly practised method [3, 7, 15], although 3-point bending has also been performed [14]. However, even when identical strength measurement methods are conducted, the test parameters often differ [3, 15], making reliable comparisons difficult.

High temperature strength may be a more relevant property since many test components will fail in service at elevated temperature. This is significant since room temperature failure mechanisms for ceramics often differ from the behaviour observed at higher temperatures. However, elevated temperature strength testing is more complex since strength is affected by many test parameters such as heating rate, test environment, stabilising period and test temperature. A test variable that is frequently overlooked is the surface condition of the corroded sample. Strength has been tested on samples with the entire corrosion product left intact [14], with the compressive face polished to provide a smooth surface [3] and with the whole oxidation scale removed by chemical etching [16]. The surface preparation of the sample prior to strength testing would be expected to have an effect on the measured values when the oxide makes a contribution towards the material's strength. Any loss of load bearing material by the corrosion treatment should not be disregarded in strength calculation.

Strength is influenced by the alteration of phase composition and morphology during oxidation. Effects such as surface roughening [17] and the relief of compressive stresses within the substrate [18] have been proposed to decrease the room temperature 4-point flexural strength of silicon nitride ceramics. Room temperature strength measurements are sensitive to the surface condition of the specimen whilst high temperature strengths are, on the other hand, influenced by the characteristics of the grain boundary phase [14, 19–21].

Silicon nitride ceramics are candidate for applications that involve the exposure to salt containing environments. The effects of sodium enhanced oxidation on the mechanical properties are therefore a concern. Alteration of the grain boundary material and the generation of pitting morphologies are the two primary mechanisms considered to decrease the strength of Si_3N_4 exposed to sodium contaminated atmospheres [3, 7]. However, a clear understanding of the details of Na attack and its effect on the mechanical properties has still to be established. Fox *et al.* [3] observed that the extent of strength deterioration increased with the Na concentration of the combustion gas, whereas Swab and Leatherman [15] reported that room temperature strength actually increased when more sodium sulphate was coated onto silicon nitride. However, the different techniques used for inducing corrosion prevent a detailed comparison between the two sets of results.

There were several objectives of this exercise. As mentioned earlier, the primary goal was to study the effect of sulphur in simulated gas turbine environments on the room temperature and 1000 °C strength of silicon nitride. The aspects of mechanical testing that may influence the strength measurements have been presented above. It is not within the scope of this investigation to elucidate the effect of each and every test parameter on the material's strength, but rather to isolate the role of the oxide scale on the sample during the mechanical test. This information should at least provide a small

contribution towards the development of standard test procedures.

2. Experimental

2.1. Material

Silicon nitride (Morgan Matroc, UK), sintered with the aid of 12.2 wt % Y_2O_3 and 5.1 wt % Al_2O_3, was studied in this investigation. This material was selected on the basis that it is a commercially available product representative of silicon nitride ceramics predicted for use at elevated temperature (the manufacturer's recommended maximum use temperature was 1300 °C). Test bars were prepared according to EN 843-1, i.e. nominal dimensions $3 \times 4 \times 50$ mm, with all four major edges chamfered and supplied in the as machined condition (0.4 R_a). Transmission electron microscopy (TEM) analysis revealed that the microstructure consisted of β-Si_3N_4 grains contained in a completely amorphous integranular phase.

In preparation for exposure in the burner rig, the dimensions of each sample were determined to ± 1 μm at 3 points along the length using a micrometer. After the length was measured to 0.1 mm with a vernier calliper, the samples were ultrasonically cleaned in ethanol, dried and then weighed on a balance accurate to 10 μg.

2.2. Corrosion

A schematic diagram of the low velocity burner rig used in this study is shown in Fig. 1. Ref. [22] offers a detailed description of this type of corrosion testing facility. The operating conditions were based on the VAMAS guidelines [9] for molten salt corrosion of superalloys. The conditions were modified, in respect of temperature, for the exposure of Si_3N_4 to salt vapours. Artificial ocean water was prepared to ASTM D1141 and then diluted 1 : 3 with distilled water [5]. This solution was delivered into the rig at 50 ml $\cdot$ h^{-1} an atomised with 552 l $\cdot$ h^{-1} of air to achieve a sodium flux of 4 mg $\cdot$ cm^2 $\cdot$ h^{-1}. The interaction of silicon nitride samples with two simulated gas turbine environments was examined at atmospheric pressure. Combustion gases were simulated by injecting either an aviation kerosene (0.01 wt % S) or a marine diesel (1 wt % S) at the rate of 72 ml $\cdot$ h^{-1} into the burner rig together with 552 l $\cdot$ h^{-1} of air.

Samples were exposed to the aviation kerosene for three 20 h cycles and to the marine diesel for one 20 h cycle. This procedure was developed to examine the effect of sulphur on the silicon nitride's mechanical properties and, by altering the quantity of reaction product formed by corrosion, the affect of the oxide thickness on the material's strength could also be evaluated. Although a direct comparison between the two conditions is not strictly accurate, it will be shown later that strength degradation does not critically depend on the corrosive environment.

The exposure temperature, 1000 °C, was sufficiently high to prevent molten salt deposition, thereby ensuring the investigation of the interaction between silicon nitride and salt vapours. Seven Si_3N_4 samples were exposed vertically to the combustion gas that flowed at approximately 0.2 m $\cdot$ s^{-1}. Each specimen was supported at the bottom by a metallic table that rotated slowly ($\sim$5 rpm) to promote uniform exposure of all sample faces. Alumina crucibles that were used to prevent direct contact between the silicon nitride test bars and the sample table also allowed for the collection of low viscosity corrosion products. Small weight changes of alumina reference samples that were simultaneously

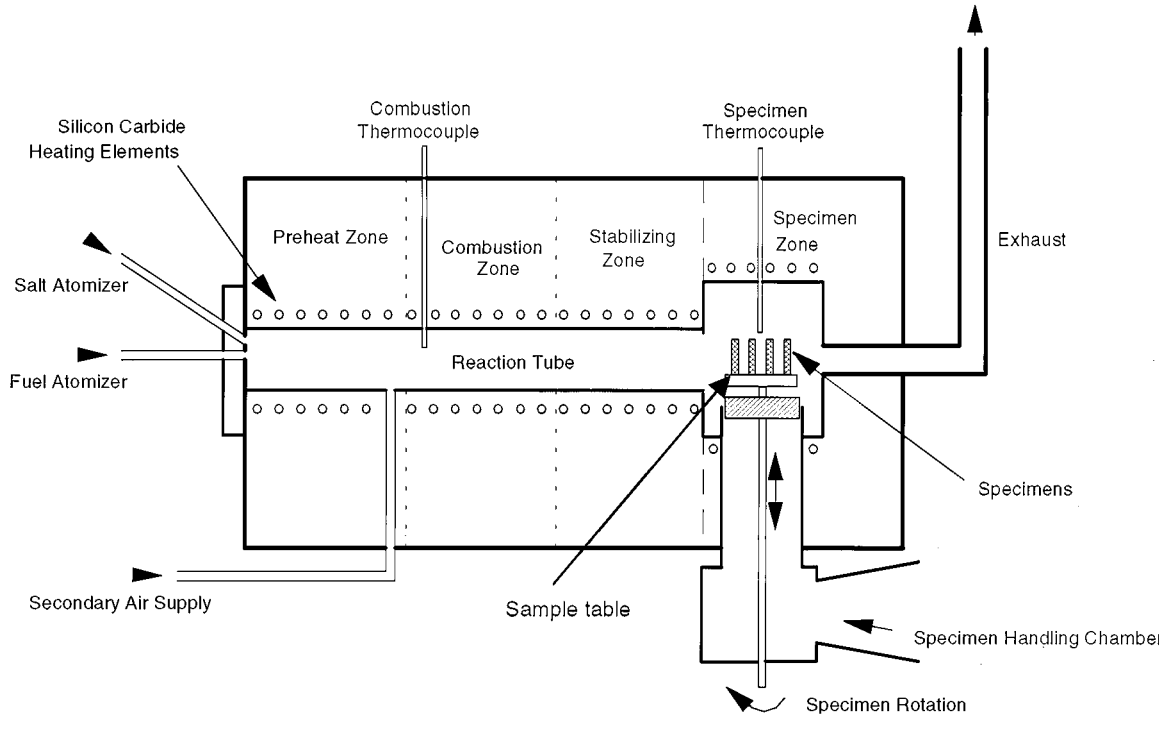

Figure 1 Schematic diagram of the low velocity, atmospheric pressure burner rig used in this study.

exposed verified that salt deposition did not occur. After each 20 cycle, the samples were removed from the combustion gas and cooled rapidly in laboratory air. Weight change was used as the initial method of evaluating the extent of corrosion.

2.3. Mechanical testing

Four-point flexural strength measurements of the as-received and corroded specimens were performed at room temperature and at 1000 °C. The load was applied at a rate of 0.5 mm/min to a jig with an inner span of 20 mm and an outer span of 40 mm in accordance with EN843-1. The jig design was such to minimise misaligned sample positioning that may otherwise affect the strength measurement. The elevated temperature mechanical tests were conducted in laboratory air, heating to 1000 °C at 25 °C/min. To ensure thermal equilibrium within the furnace, the samples were held at the test isotherm for 10 min before the load was applied. Certain samples had their corrosion product removed by chemical etching in a 10% HF solution at 70 °C for 2 h [7] to allow an examination of the contribution of the oxide towards strength. Although the HF treatment appeared to dissolve a very small quantity of intergranular phase, this effect is later suggested not to markedly influence strength. Seven samples were tested, unless otherwise indicated, for each experimental condition shown in Table I.

Strength (σ_f') was determined using the test bars' original dimensions. Thus the oxide thickness was not considered in the strength calculation so that the effects of surface recession or oxide growth are reflected in the material's loading bearing capacity (engineering design strength).

After the mechanical test, all fractured pieces were recovered and photographs of fracture surfaces were taken to identify the origin of failure. Scanning electron microscopy (SEM) and energy dispersive X-ray (EDX) analysis was performed on the corroded surfaces of samples exposed to both combustion environments to compare the corrosion products' chemical composition and morphology. The surfaces of samples that had their corrosion product removed by HF were also examined. This was to provide details of the attack morphology. The SEM was also used to focus attention on the suspected fracture origins to identify if chemical or geometrical features were involved in the failure mechanism.

3. Results and discussion

3.1. Mechanical properties of the as-received silicon nitride

A summary of the room temperature 4-point bend strengths of the as-received and corroded test bars is shown in Table II. The average strength of as-received material (496.4 $N \cdot mm^{-2}$) is low compared with 585 $N \cdot mm^{-2}$ of a similar sintered silicon nitride (13 wt % Y_2O_3, 3 wt % Al_2O_3) tested under essentially identical conditions [23].

Processing flaws were the most commonly observed source of fracture. Improper densification resulted in localised areas of porosity (Fig. 2), the characteristics of which varied considerably from one test bar to another. The large scatter in the data is attributed to variations in the size, shape and location of these critical defects.

The strength at 1000 °C is approximately 20% lower than that measured at room temperature. Also the standard deviation of strength values are lower at 1000 °C than at 20 °C. These effects are attributed to slow crack growth taking place during the high temperature test from a sub-critical defect. Fig. 3a is a typical example of the involvement of slow crack growth in the failure process. Slow crack growth likely leads to the generation of more uniform critical defect characteristics. A similar shape factor, Y, of the critical defect lends to the decreasing standard deviation of strength values at 1000 °C. Although slow crack growth was the most commonly observed failure mechanism, large surface defects were identified as the fracture origin in several samples that showed no characteristics of slow crack growth (Fig. 3b). Thus, slow crack growth is likely to operate when the size of the manufacturing flaws are sub-critical.

The mechanical performance of the as-received silicon nitride, both at room temperature and at 1000 °C, is strongly influenced by processing defects. The samples are inhomogeneous in terms of microstructure, with uneven distribution of the intergranular phase resulting in localised areas of low density. These regions were identified as the most frequent source of room temperature failure and are responsible for the low strengths. The differences in the characteristics of defects introduced during manufacture, namely shape, size orientation and location, resulted in large scatter in the silicon nitride's strength. The elevated temperature strength is less dependent on manufacturing defects present at/or near the tensile surface and is affected more by the

TABLE I Corrosion and mechanical testing experimental conditions

Burner rig testing			Mechanical testing	
SET	Fuel (wt % S)	Time (h)	Temperature (°C)	Surface condition
As received	—	—	RT	As received
As received	—	—	1000	As received
A	0.01	60	RT	Entire scale removed
B	0.01	60	RT	As corroded
C	0.01	60	1000	Entire scale removed
D	1	20	RT	As corroded
E	1	20	1000	As corroded

TABLE II Effect of corrosion on room temperature 4-point flexural strength ($N \cdot mm^{-2}$)

Fuel (% S)	—	0.01	1	0.01
Surface condition	As-received	As-corroded	As-corroded	Washed
SET	—	B	D	A
Samples tested	8	7	7	7
Average strength (σ_f')	496.36	366.60	423.11	304.97
Standard deviation	82.65	58.63	108.54	85.41
$\sigma_f'/\sigma_{f(ASREC)}'$ (%)	100.00	73.86	85.24	61.44

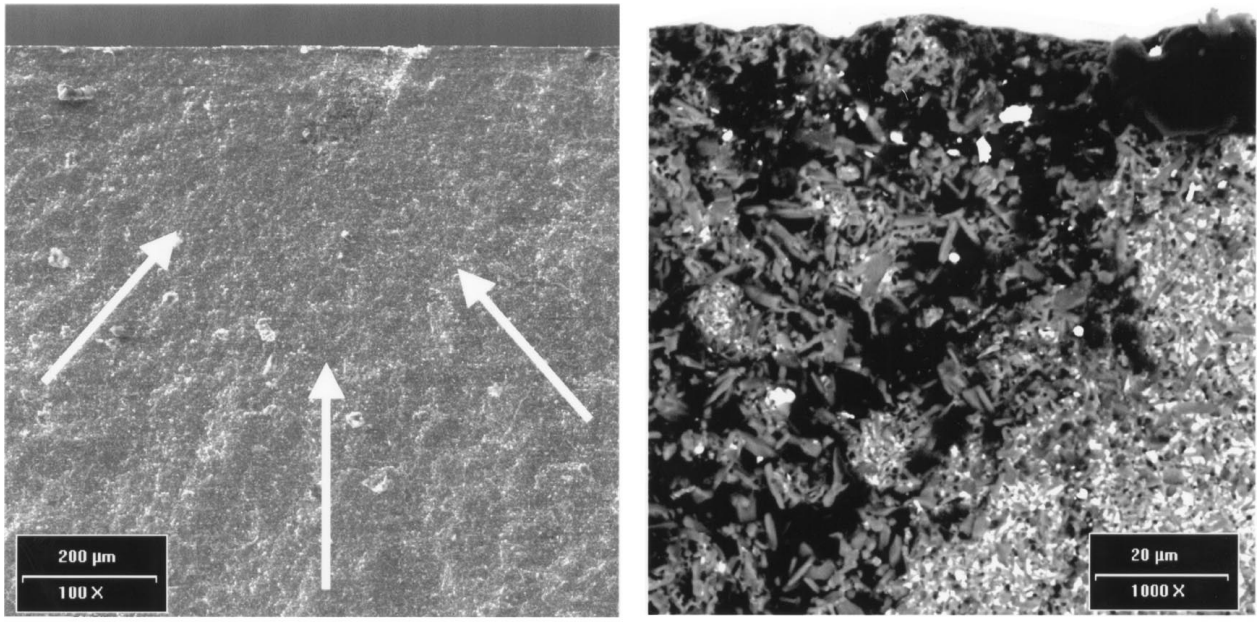

(a) (b)

Figure 2 (a) SEM image showing the most frequently observed source of failure (an internal flaw) for as-received test bars and (b) the higher magnification back scattered electron (BSE) image reveals the presence of Si_3N_4 grains not surrounded by an intergranular phase.

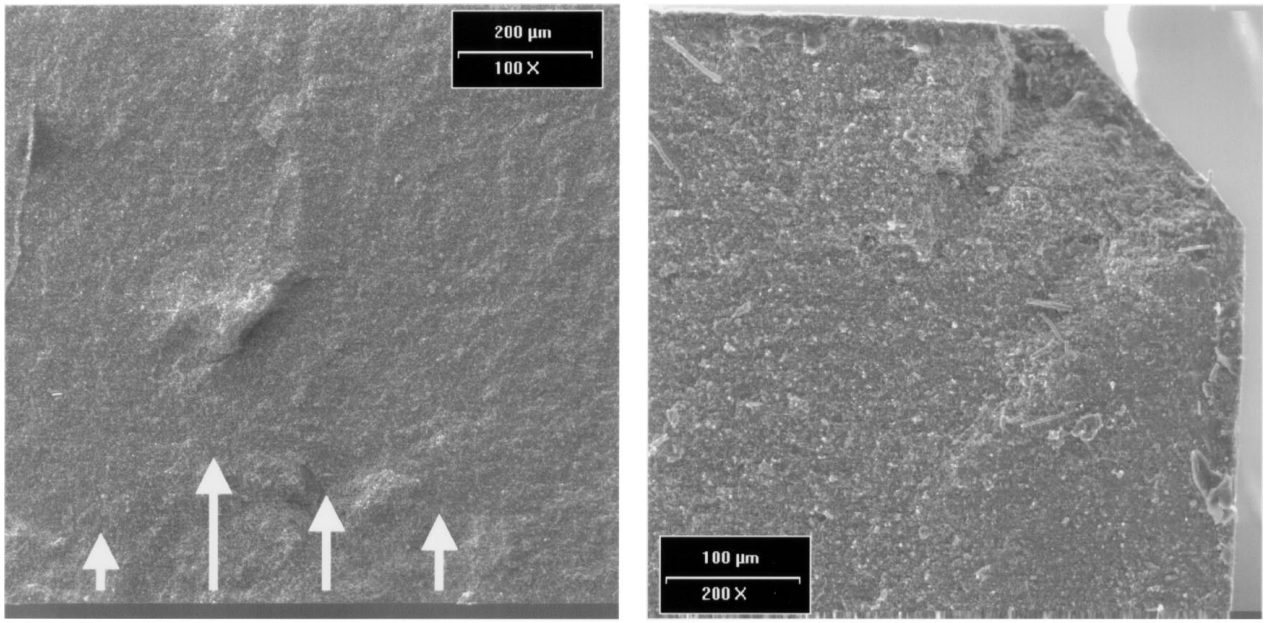

(a) (b)

Figure 3 Origins of failure under 4-point bending at 1000 °C of two different as-received test bars. The arrows in (a) highlight the development of slow crack growth away from the tensile surface. The fracture origin in (b) is at the corner of the specimen, the tensile surface being the top edge. The characteristics of the flaw are typical of a manufacturing defect.

characteristics of the intergranular phase and by slow crack growth during the test. Since slow crack growth proceeds until the critical flaw size is exceeded, less scatter is observed in the 1000 °C strength.

3.2. Weight change of the corroded silicon nitride

The weight change of the silicon nitride during exposure in the burner rig is shown in Fig. 4. The effect of increasing the sulphur content of the fuel on corrosion is clearly demonstrated. Weight gains measured after 20 h exposure to the low P_{SO_3} environment were over six times greater than that in the high P_{SO_3} combustion gas (1×10^{-2} and 2 $kg \cdot s^{-2} \cdot m^{-1}$, respectively [24]) after the same time period. The kinetic behaviour in the 0.01 wt % S environment is best described by a linear function with respect to time. This implies that an interfacial reaction may be controlling the overall corrosion process. Kinetic analysis of corrosion in the

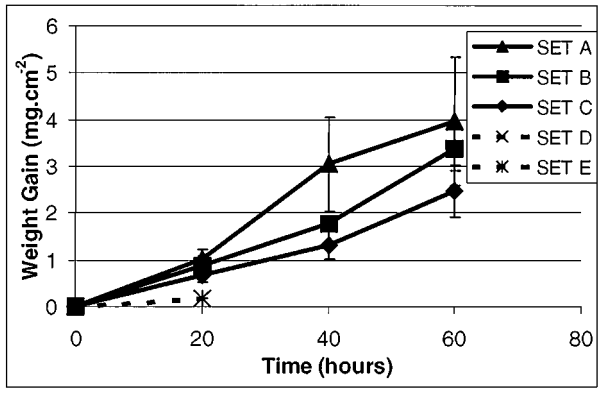

Figure 4 Corrosion of the silicon nitride at 1000 °C in the simulated gas turbine environments expressed as an average weight change of the seven samples. Samples in sets A–C were exposed to the 0.01 wt % S fuel, whereas samples in sets D and E were exposed to the 1 wt % S fuel. The error bars represent ±1 standard deviation of the seven measurements.

1 wt % S gas is prevented since only one thermal cycle was completed to ensure formation of a thin reaction product.

The weight gains of all 14 samples exposed to the 1 wt % S gas after two separate thermal cycles were comparable (0.18 ± 0.01 mg $\cdot$ cm^{-2}). This obstructs distinguishing the data points of SETS D and E in Fig. 4. In contrast, there existed large variations in the corrosion rates between samples exposed to the 0.01 wt % S combustion environment. Although there was no significant difference between the average weight gain of samples in SETS B and C, the results obtained from SETS A and C were significantly different. The large scatter in the results from SET A was due primarily to the markedly higher weight gains of the two samples located either side of the alumina reference samples. This effect was not evident during the other two tests. The poor reproducibility observed between different runs is attributed to small variations in the fuel and salt fluxes.

3.3. Microstructural analyses of the corrosion products

There existed major differences between the features of the corrosion products formed in the two combustion environments, as expected. A dense amorphous corrosion product of uniform thickness ($\sim$3 μm) adhered well to the silicon nitride exposed to the 1 wt % S gas after 20 h. EDX analysis suggested that the corrosion product was a silica glass containing Y, Al and Na contamination. Topographical micrographs obtained using the BSE beam identified that crystals (characterised as yttrium silicates by X-ray diffraction) as well as small bubbles were present in the glass. The morphology and chemical composition of the corrosion product formed in the 1 wt % S gas contrasts with that observed after 60 h exposure to the 0.01 wt % S environment. A porous layer of non-uniform thickness, up to 250 μm thick in places, was present that poorly adhered to the underlying substrate. The characteristics of the corrosion product suggested that it existed as a low viscosity glass during exposure in the burner rig. SEM examination of the surface revealed that the layer was primarily amorphous. Although the oxide chemistry was similar to that formed in the 1 wt % S gas, semi-quantitative EDX analysis indicated that the corrosion product formed in the 0.01 wt % S environment contained more Na. BSE images suggested the presence of isolated Si_3N_4 grains in the glass, together with unevenly dispersed regions rich in yttrium. The differences in the oxide characteristics between the two sulphur gases are appropriate for assessing the role of the scale on strength.

Further information regarding the corrosion attack mechanism in the 0.01 wt % S gas can be obtained from microscopy of the samples after HF etching. SEM analyses of the surface topography revealed there existed less intergranular phase, exposing many protruding Si_3N_4 grains, in the corroded sample compared with that observed on a similarly etched as-received specimen. This difference may be a result of the grain boundary material being preferentially attacked by corrosion or the formation of an intergranular phase-depleted zone adjacent to the substrate due to the outward diffusion of cations to the scale [25].

Corrosion, defined by both weight change data and the microstructural examination, is more severe in the 0.01% S combustion gas. This behaviour is similar to that of SiC exposed under identical conditions in a previous exercise [6]. Thus, it is likely that a similar corrosion mechanism operates for both materials exposed to these combustion environments. The effect of lowering the sulphur content of the fuel is to increase the basicity of the gas, thereby increasing the activity of the sodium bearing species in the combustion environment. The acidic silica layer that normally forms on silicon based ceramics is modified by the incorporation of sodium from the combustion environment. This contamination lowers the glass viscosity, allowing faster oxygen transport towards the bulk material so that the Si_3N_4 is oxidised at a faster rate. The conversion of more Si_3N_4 to SiO_2 results in faster section loss.

3.4. Mechanical properties of the corroded silicon nitride

The effect of corrosion is to degrade the silicon nitride's average room temperature 4-point bending flexural strength, the extent of which is greater in the 0.01 wt % S environment (Table II). This is in agreement with the weight change measurements, although the magnitude of the effect of corrosion is not as great by 4-point flexural strength testing. The average strength (σ_f') of the as-corroded silicon nitride after exposure to the 0.01 wt % S gas for 60 h is $\sim$90% of that exposed to the 1 wt % S gas for 20 h. In contrast, weight change measurements indicate that corrosion is between 10–20 times more severe in the 0.01 wt % S combustion environment. Moreover, the average strength after corrosion is not statistically different from the as-received strength, as well as, the strengths of the silicon nitride test bars exposed to the different combustion gases.

The effect increasing time and decreasing P_{SO_3} leading to higher weight gains is not reflected in the Si_3N_4 strength degradation. Since it is unreasonable to suggest that higher strengths could result from exposure to the more aggressive gas, an indirect strength comparison

between 20 and 60 h exposure to the 1 and 0.01% S gas, respectively, is possible. Even if a mechanism operates that imparts better strength in the 0.01% S gas, it is clear that the difference in Si_3N_4 corrosion between the two sulphur gases is not as great by strength measurement than by weight change assessment.

Although there existed large differences in the corrosion products formed in both combustion gases, fractography did not identify variations in the process controlling the silicon nitride strength after corrosion. Thus the fractography results presented herein relate to silicon nitride exposed to both gas turbine environments.

Different types of fracture origins were identified after corrosion. However, corrosion induced flaws were not typically responsible for failure. The primary source of failure of the corroded samples was similar to that observed in the as-received silicon nitride, namely areas of porosity caused by poor intergranular phase distribution (Fig. 5). These critical defects were located at/or near the tensile surface. Variations in the characteristics of these flaws resulted in scatter in the strength data.

Strength control by internal processing defects to either combustion gas can explain the negligible effect of corrosion on strength. Corrosion is a surface phenomena, caused by the interaction between the silicon nitride and the environment. Although the effect of sulphur content is reflected in the weight change data, the extent of corrosion is not significant to modify or create new defects with characteristics more critical than the flaws already existing from manufacture. This explains the limited effect of corrosion on strength.

The role of corrosion, modifying the surface topography of the silicon nitride, on strength may be investigated further. A poorly densified region was responsible for failure in a silicon nitride test bar that contained a pit at the tensile surface. The strength of this sample (Fig. 5) was $\sim 50\ \ \mathrm{N \cdot mm^{-2}}$ lower than the average value. A pit was identified as the fracture origin in another test bar, but the strength was $\sim 60\ \mathrm{N \cdot mm^{-2}}$ higher than the average. These aspects demonstrate that alteration of the silicon nitride's surface by corrosion does not necessarily play a critical role in the material's room temperature strength.

Corrosion may modify the bulk microstructure of the silicon nitride by internal oxidation. There were two instances when porous regions extended to the outer material surface, allowing internal oxidation to occur. However, the fracture origin in both cases was a poorly densified area located away from the area affected by oxidation. This supports the view that defects introduced during manufacture generally have more influence on strength than those modified or created by internal oxidation or corrosion. A region affected by corrosion may only act as the source of failure when it is more critical than other manufacturing flaws present in the material. Corrosion in this study is not significant to satisfy this condition, thus the silicon nitride's room temperature strength, even after exposure to combustion environments, is controlled primarily by defects introduced during manufacture.

The effect of the oxide layer on the silicon nitride strength is now examined. Treatment of as-received SiC to a similar washing procedure used in this study has been reported to result in a significant decrease in strength [7]. The limited number of test bars available for this investigation prevented such an assessment being made for the silicon nitride. Table II highlights the differences in room temperature strength between two sets of samples exposed to the 0.01 wt % S gas environment; one set was tested in the as-corroded condition, whilst the other had its corrosion product removed by the HF treatment prior to mechanical testing. The

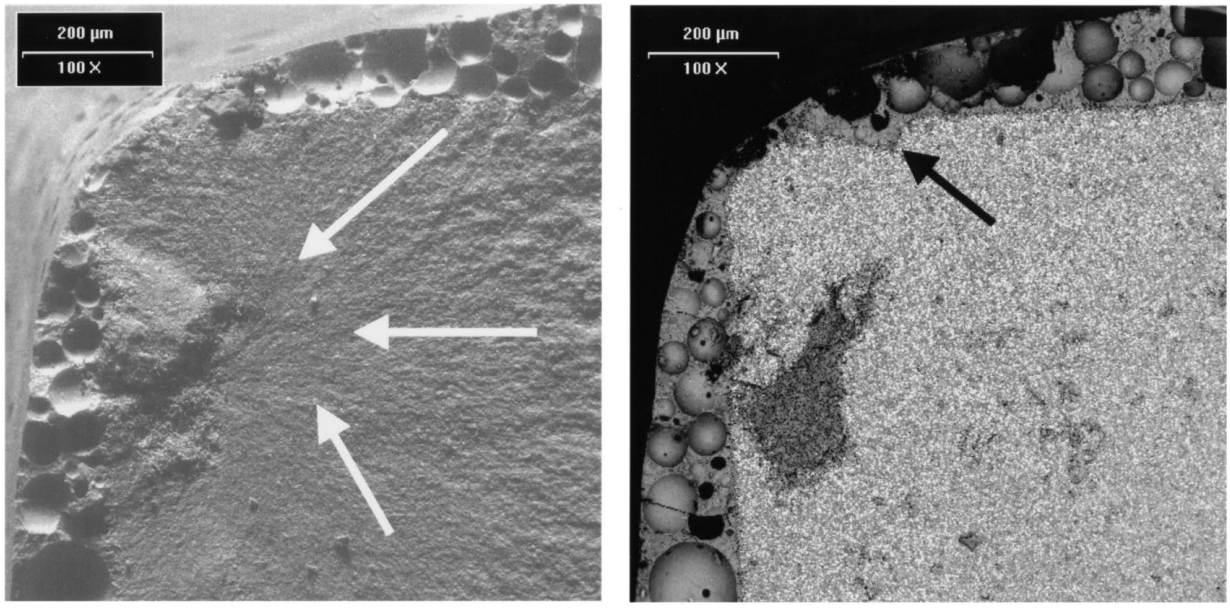

(a) (b)

Figure 5 Fracture origin of a test bar fractured at room temperatures after exposure to the 0.01 wt % S combustion gas for 60 h: (a) the striations point towards an internal flaw 400 μm beneath the tensile (top) surface and (b) the BSE image shows that the crack responsible for failure has propagated from a point close to the edge of a large area of low intergranular phase concentration. Notice that the pit (black arrow) on the tensile surface does not appear to influence the test bar's failure mechanism.

average strength of the washed samples was lower with a higher standard deviation (305.0 ± 85.4 N $\cdot$ mm^{-2}) compared with the strength of the as-corroded silicon nitride (366.6 ± 58.6 N $\cdot$ mm^{-2}). The washed samples could be placed easily in the jig since all surfaces were uniformly smooth, whereas there existed difficulty in positioning the as-corroded samples due to the irregular shape of the corrosion product. Misalignment may have been a source for scatter in the strength data but this is inconsistent with the results since the standard deviation in strength of the as-corroded tests bars was lower than that calculated for the washed samples.

Comparing the silicion nitride surfaces of the washed and as-corroded test bars, an intergranular phase depleted zone ($\sim$20 μm) was observed after washing. However, the fracture origin did not exist in this zone, in any of the test bars. Thus it appears likely that neither the HF treatment nor the modification of the grain boundary phase by the corrosion process has deteriorated the silicon nitride's room temperature flexural strength.

Three washed test bars primarily account for the scatter and low average flexural strength. Areas of low intergranular phase concentration at or close to the tensile surface were identified as the fracture origin in these samples. Therefore, it is believed that differences in the features of areas of poor densification are primarily responsible for the variations in strength between the washed and corroded samples.

Although HF washing led to the dissolution of some intergranular phase at the surface, flaws thereby created were less critical than the manufacturing defects. Since alignment of the washed samples in the jig was easier, it is recommended that porous, non uniform corrosion products are chemically dissolved prior to mechanical testing. However, great care must be exercised, especially in the case of homogeneous engineering ceramics, since this procedure may introduce critical flaws.

TABLE III Effect of corrosion on the 1000 °C 4-point flexural strength (N $\cdot$ mm^{-2})

Fuel (% S)	—	1	0.01
Surface condition	As-received	As-corroded	Washed
SET	—	E	C
Samples tested	6	7	7
Average strength (σ_f')	398.59	400.35	349.24
Standard deviation	66.70	35.18	61.59
$\sigma_f'/\sigma_{f(ASREC[1000\,^\circ C])}'$ (%)	100.00	100.44	87.62
$\sigma_f'/\sigma_{f(ASREC)}'$ (%)	80.30	80.66	70.36

Elevated temperature strength depends less on the surface morphology of the test bar and more on the characteristics of the material's intergranular phase. Therefore less influence of corrosion induced surface flaws is expected on the 1000 °C flexural strength. Table III highlights that the 1000 °C strength is not significantly affected after exposure to either combustion gas. Slow crack growth was commonly identified as the strength controlling mechanism (Fig. 6a). However no features typical of slow crack growth were evident in other samples that contained large manufacturing defects (Fig. 6b). This behavior is similar to that observed for the 1000 °C strength of the as-received silicon nitride. Slow crack growth takes place in samples that contain only sub-critical flaws. A slow crack growth process is not involved in the strength mechanism in samples containing manufacturing defects larger than the critical defect size. There was no evidence to suggest that sub-critical cracks propagate from corrosion induced flaws. Thus, 1000 °C strength of silicon nitride after corrosion is controlled primarily by the presence of defects introduced during manufacture.

Elevated temperature testing is sensitive to the attack of the grain boundary material and thus any effect in the modification of the intergranular phase by

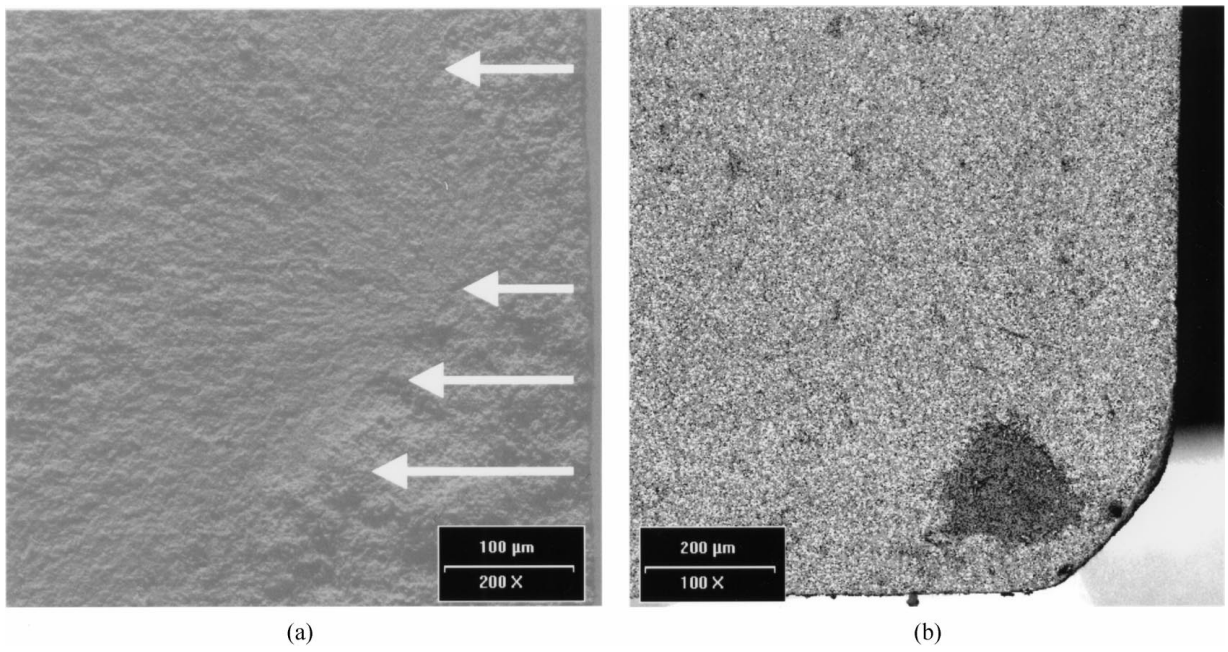

Figure 6 Fracture origins of two test bars exposed to the 0.01 wt % S gas, washed in HF and then mechanically tested at 1000 °C. The slow growth area is visible on the tensile surface of the secondary electron image (a), whilst an area of low density was responsible for failure in a different sample (BSE image b).

sodium during corrosion is more likely to be observed on the material's 1000 °C flexural strength. However, since there is no appreciable deterioration in the elevated temperature strength in either set of corroded samples, it appears that any alteration of the intergranular phase has not adversely affected the silicon nitride's behaviour. Fractography did not identify that the preferential attack of the intergranular phase acted as a source of failure. Therefore the silicon nitride's strength at 1000 °C, similarly to the room temperature strength, is not significantly affected by corrosion, in contrast to the weight change results.

There does not appear to be a difference in the strength limiting effect after corrosion from that observed in the as-received silicon nitride. At room temperature large inhomogeneities, which differ greatly in size and shape, are strength limiting defects, whereas at 1000 °C slow crack growth and the properties of the intergranular phase play an important role in strength. This demonstrates that exposure of this silicon nitride to simulated gas turbine environments has neither significantly affected the fracture mechanism nor the material's strength, highlighting the importance of developing the material's microstructure during manufacture to optimise its mechanical properties.

4. Conclusions

Reducing the P_{SO_3} of the combustion gas resulted in larger silicon nitride weight gains due to the enhanced formation of reaction product. However, the effect of sulphur concentration on strength degradation was not as significant. Processing flaws were identified as the principal strength controlling defects in the as-received and corroded silicon nitride. The insensitivity of strength to modification of the surface layer by corrosion coincided with the presence of large processing flaws in the bulk material. The temperature of the strength test influenced the failure mechanism and the extent of strength degradation by corrosion.

The oxide scale did not appear to significantly influence the silicon nitride's strength, although a clear understanding of the effect is prevented by the poor microstructure of the silicon nitride.

This study highlighted the disparity that can exist between the assessment of corrosion by weight change information/microstructural characterisation of the corrosion product and strength testing. The discrepancies between the effect of sulphur on silicon nitride performance to simulated gas turbine environments by weight change and strength has resulted from the poor microstructure of this commerically available material. Selection of a component system, i.e. material and environment, purely on the basis of weight change or scale thickness measurements is therefore a great concern.

Acknowledgements

The authors wish to thank A. Zato for his contribution towards performing the burner rig tests. The assistance provided by I. Goded and B. Fischer to conduct the strength tests is also gratefully appreciated. This work has been carried out within the European Commission's Research and Development Program in collaboration with the University of Strathclyde, Glasgow.

References

1. D. FOX and J. SMIALEK, *J. Amer. Ceram. Soc.* **73** (1990) 303.
2. T. GRAZIANI, D. BAXTER and A. BELLOSI, *J. Mater. Sci.* **32** (1997) 1631.
3. D. FOX, M. CUY and T. STRANGMAN, *J. Amer. Ceram. Soc.* **80** (1997) 2798.
4. D. MCKEE and D. CHATTERJI, *ibid.* **59** (1976) 441.
5. N. S. JACOBSON, *Oxid, Metals* **31** (1989) 91.
6. M. CARRUTH, D. BAXTER, F. OLIVIRA and K. COLEY, *J. Euro. Ceram. Soc.* **18** (1998) 2331.
7. J. SMIALEK and N. JACOBSON, *J. Amer. Ceram. Soc.* **69** (1986) 741.
8. C. JUST, "High Temperature Alloys for Gas Turbines" (Applied Science Publishers, London, 1978) p. 146.
9. S. SAUNDERS and J. R. NICHOLLS, *High Temperature Technology* **7** (1989) 232.
10. L. WANG, C. HE and J. WU, *Mater. Sci. & Eng.* **A157** (1992) 125.
11. P. ANDREWS and F. RILEY, *J. Euro. Ceram. Soc.* **7** (1991) 125.
12. J. PERSSON and M. NYGREN, *ibid.* **13** (1994) 467.
13. K. G-AHARI, K. S. COLEY and J. R. NICHOLLS, *ibid.* **17** (1997) 681.
14. C. HE, L. WANG and J. WU, *J. Mater. Sci.* **28** (1993) 4829.
15. J. SWAB and G. LEATHERMAN, *J. Euro. Ceram. Soc.* **5** (1990) 333.
16. J. HAGGERTY, A. LIGHTFOOT, J. RITTER, P. GENNARI and S. NAIR, *J. Amer. Ceram. Soc.* **72** (1989) 1675.
17. M. MAEDA, K. NAKAMURA, T. OHKUBO, I. ITO and E. ISHII, *Ceram. Int.* **15** (1989) 247.
18. T. STRANGMAN and D. FOX, AGARD-CP-558, Canada Communications Group, Quebec, November 1994, pp. 36-1-11.
19. S. KNICKERBOCKER, A. ZANGVIL and S. BROWN, *J. Amer. Ceram. Soc.* **68** (1985) C99.
20. M. CINIBULK, G. THOMAS and S. JOHNSON, *ibid.* **73** (1990) 1606.
21. J. SHELBY, S. MINTON, C. LORD and M. TUZZOLO, *Phy. Chem. Glasses* **33** (1992) 93.
22. M. CARRUTH, D. BAXTER and K. COLEY, in "Euro Ceramics V, Part 3," *Key Engineering Materials* **132–136** (Proceedings of the 5th Conference of the European Ceramic Society, June 1997, edited by D. Baxter *et al.* (Trans Tech Publications)) p. 1645.
23. G. QUINN and W. BRAUE, *J. Mater. Sci.* **25** (1990) 4377.
24. G. ERIKSSON, *Chemica Scripta* **8** (1975) 100.
25. G. BABINI, A. BELLOSI and P. VINCENZINI, *J. Mater. Sci.* **19** (1984) 1029.

Received 5 August 1998
and accepted 26 March 1999